Journal of the Korean Nuclear Society
Volume 23, Number 3, September 1991

Analysis of Secondary Flow Effects on Turbulent Flow in Nuclear Reactor Fuel Rod Bundles

Jae-Yeong Shon and Goon-Chul Park
Seoul National University
(Received July 12, 1990)

핵연료 집합체 내에서의 이차유동이 난류에 미치는 영향에 대한 해석적 분석

손재영 · 박군철
서울대학교
(1990. 7. 12 접수)

Abstract

It is important to predict the main feature of fully developed turbulent secondary flow through infinite triangular arrays of parallel rod bundles. One-equation turbulence model which include anisotropic eddy viscosity model was applied to predict the exact velocity field. For a constant properties, Reynolds equations were solved by the finite element method. Mean axial velocity near the wall is simulated by the law of the wall. The numerical results showed good agreement with avaiable experimental data. The strength of the secondary flow increased with Reynolds number but decreased with rod spacing, P/D (pitch-to-diameter). The secondary flow affects remarkably the distribution of the axial velocity, wall shear stress and turbulent kinetic energy in the closely packed rod array bundles.

요 약

핵연료봉의 정방형 또는 삼각형 배열내의 2차 난류 유동의 해석은 연료봉내의 온도분포와 열전달 과정의 해석에 있어서 중요한 문제이다. 비등방성 난류모델과 등방성 난류모델을 사용하여 속도장을 구하였고 열수력학적 성질이 일정하다는 가정하에 지배방정식을 유한 요소법을 사용하여 수치해석적인 방법으로 해를 구하였다. 또한 연료봉 표면 근처에서는 유체의 유동이 난류가 아니기 때문에 축 방향 속도는 벽의 법칙에 의해서 계산하였다. 이러한 방법에 의해서 구해진 해는 실험 결과와 비교되었고 비교적 잘 일치하였다.

1. Introduction

Most nuclear power reactors have fuel bundles which consist of a parallel matrix of rods arranged mainly in triangular and square arrays. In the space between the rods, the coolant flows axially through the bundles. It is important to predict the exact velocity distributions of the fluid which are input data for accurate calculation of the temperature field. However, it is very difficult to analyze the flow phenomena due to the complex turbulent phenomena in such closely-packed geometry, where the secondary flows are very active. Re-

cently, the phenomena of secondary flow have received increasing attention because heat transfer is enhanced by it. However, current design methods are usually based on a subchannel mixing technology which involves subchnnel–average quantities and does not explictly recognize the secondary flows.

Therefore in this work, the secondary flow in infinite triangular arrays of the parallel rods is analyzed by the one–equation turbulence model. Anisotropic eddy viscosity is considered by introducing the different length scale for the eddy viscosity normal and parallel to the wall. In the analysis of turbulent secondary flow velocity distribution, the Reynolds stress model proposed by Launder and Ying is used. To find the numerical solutions of the governing equation, the finite element method is adopted and the integral form of the governing equations are constructed by the Galerkin's weighted residual method, where the weighting function is the same as the shape function. The numerical results are compared with the available data. And this work calculates shear stress distribution, secondary flow velocity field, axial velocity field, turbulent kinetic energy and friction factor by varying Reynolds number and P/D (pitch–to–diameter). The isotropic and anisotropic effects are included in the analysis of velocity distribution.

2. Turbulence Model

Among the various models of the turbulent flow in the nuclear rod bundles, the present numerical predictions are a continuation of rod bundle work initiated in 1966 by Trupp and Azad in which a wide–ranging experimental study was conducted on the equilateral triangular rod bundles arrays. [1] Since that time, a related study was undertaken in which fully–developed turbulent flow was explored experimentally for a triangular duct. The measured secondary flows are successfully predicted using the Launder–Ying model. For the turbulence model of this work, the one–equation turbulence model is adopted where the Reynolds stress can be expressed in terms of axial velocity gradient and eddy viscosity based on turbulent kinetic energy by Kolmogorov– Prandtl turbulent kinetic energy hypothesis. [3] Local turbulent phenomena are dependent on local length scale and turbulent kinetic energy due to fluctuations of the turbulent flow.

The transport equation of the turbulent kinetic energy equation construct the one–equation where the length scale can be obtained algebraically. In this model, eddy viscosities are important parameters to predict flow phenomena in the complex geometry. Experiments have shown that the effects of the anisotropic eddy viscosity play an important role on the flow and heat transfer mechanism. Thus in this study the effect of the anisotropy is considered by regarding it as a function of length as well as direction to the wall. [4] Slagter's description for the length scale is used, which depends on locus as well as direction from the wall, and was deduced from experimental correlation of Carajilescov and Todreas [4]. And in the vicinity of the wall, the velocity field is analyzed by the wall function because the pattern of flow is laminar.

3. Governing Equation

A primary flow cell for rod bundle arrays is shown in Figure 1 together with the rectangluar coordinate system (x,y,z) used in the investigation. The fundamental equations for the computation of velocity field in any geometry are the Navier–Stoke's equation and continuity equation. For fully developed turbulent flow with a constant thermal properties of fluid, the Reynolds equation are gievn by the following equations.

(a) X–directional momentum equation ;

$$\rho\left(V\frac{\partial V}{\partial x}+W\frac{\partial V}{\partial y}\right)=-\frac{\partial P}{\partial x}+\mu\left(\frac{\partial^2 V}{\partial x^2}+\frac{\partial^2 V}{\partial y^2}\right)-\rho\left(\frac{\partial \overline{v^2}}{\partial x}+\frac{\partial \overline{vw}}{\partial y}\right) \quad (1)$$

(b) Y–directional momemtum equation ;

$$\rho\left(V\frac{\partial W}{\partial x}+W\frac{\partial W}{\partial y}\right)=-\frac{\partial P}{\partial y}+\mu\left(\frac{\partial^2 W}{\partial x^2}+\frac{\partial^2 W}{\partial y^2}\right)-\rho\left(\frac{\partial \overline{vw}}{\partial x}+\frac{\partial \overline{w^2}}{\partial y}\right) \quad (2)$$

(c) Z–directional momentum equation ;

$$\rho\left(V\frac{\partial U}{\partial x}\right)+W\frac{\partial U}{\partial y}\right)=-\frac{\partial P}{\partial z}+\mu\left(\frac{\partial^2 U}{\partial x^2}+\frac{\partial^2 U}{\partial y^2}\right)-\rho\left(\frac{\partial \overline{uv}}{\partial x}+\frac{\partial \overline{uw}}{\partial y}\right) \quad (3)$$

(d) Continuity equation ;

$$\frac{\partial V}{\partial x}+\frac{\partial W}{\partial y}=0 \quad (4)$$

where the notations are conventional, and $\frac{\partial P}{\partial z}$ is independent of x and y direction and constant in the cross–sectional area. In the above Reynolds equations, Launder and Ying have proposed Reynolds stress employing the following simple equations.

$$-\rho\overline{uv}=\mu_{11}\frac{\partial U}{\partial x} \quad (5)$$

$$-\rho\overline{uw}=\mu_{22}\frac{\partial U}{\partial y} \quad (6)$$

$$\overline{v^2}=-Cl_\mu^2\left[\left(\frac{\partial U}{\partial x}\right)^2\right] \quad (7)$$

$$\overline{w^2}=-Cl_\mu^2\left[\left(\frac{\partial U}{\partial y}\right)^2\right] \quad (8)$$

$$\overline{vw}=-Cl_\mu^2\left[\left(\frac{\partial U}{\partial x}\right)^2\left(\frac{\partial U}{\partial y}\right)^2\right] \quad (9)$$

where μ_{11} and μ_{22} are anisotropic eddy viscosities and C is an assignable turbulent constant and l_μ is length scale. Substituting equation (6) to (7) into equation (3) yields following equation.

$$\left(V\frac{\partial U}{\partial x}+W\frac{\partial U}{\partial y}\right)=-\frac{1}{\rho}\frac{\partial P}{\partial z}+\frac{\partial}{\partial x}\left[(\nu+\mu_{11})\frac{\partial U}{\partial x}\right]+\frac{\partial}{\partial y}\left[(\nu+\mu_{22})\frac{\partial U}{\partial y}\right] \quad (10)$$

Kolmogorov–Prandtl turbulent energy hypothesis is adopted to evaluate the eddy viscosity. In this hypothesis, the eddy viscosity is related to the local values of the turbulence length scale l and the turbulent kinetic energy by the following equation.

$$\mu_j=C_j\rho k^{1/2}l_{\mu j} \quad (11)$$

where C_j is constant. And the turbulent kinetic energy equation is given by the following equation.

$$\frac{\partial}{\partial x}\left[\left(\nu+\frac{\mu_{11}}{\sigma_k}\right)\frac{\partial k}{\partial x}\right]+\frac{\partial}{\partial y}\left[\left(\nu+\frac{\mu_{22}}{\sigma_k}\right)\frac{\partial k}{\partial y}\right]-C_d l_d^{-1}k^{3/2}+\mu_{11}\left(\frac{\partial U}{\partial x}\right)^2+\mu_{22}\left(\frac{\partial U}{\partial y}\right)^2=V\frac{\partial k}{\partial x}+W\frac{\partial k}{\partial y} \quad (12)$$

where C_d is the turbulent constant, σ_k is a turbulent Prandtl number for kinetic energy tranport, l_d is a length scale and μ_{11}, μ_{22} are eddy viscosity in the direction normal and parallel to the wall. It is necessary to model the eddy viscosity which needs the length scales in solving above governing equations. Wolfshtein's description for the length scale l_μ and l_d are given by the following equations.

$$l_\mu=x_l\left[1-exp\left(-A_\mu R\right)\right] \quad (13)$$

$$l_d=x_l\left[1-exp\left(-A_d R\right)\right] \quad (14)$$

where A_μ and A_d are constants and x_l is the distance from the wall. R is local turbulent Reynolds number which is defined by the following equation.

$$R = \frac{\rho x_l k^{1/2}}{\mu} \quad (15)$$

Slagter proposed anisotropic length scale model, which depends on locus as well as direction from the wall and was deduced from the experimental correlation of Carajilescov–Todreas.

The length scale of turbulent viscosity normal to the wall is given by the following equation.

$$l_{\mu,1} = x_l [\, 1 - exp\,(-A_\mu R)\,], \quad \text{for } x_l < 0.25\,\hat{x}_l$$

$$l_{\mu,1} = x_l \{\, 0.25 + 0.066 sin\, [\, (\frac{\pi}{0.55}) \, ((\frac{x_l}{\hat{x}_l}) - 0.25)\,]\,\},$$

and the length scale of turbulent eddy viscosity for the parallel to the wall is given by the following equation.

$$l_{\mu,2} = x_l [1 - exp(-A_\mu R)] \quad (17)$$

where $\hat{x}_l$ is the profile length denoting the normal distance from the wall to the position of the maximum velocity. The eddy viscosity in the direction normal to the wall was modeled by the following equation.

$$\mu_{11} = C_1 \rho k^{1/2} l_{\mu,1} \quad (18)$$

And the eddy viscosity in the direction parallel to the wall is given by the following equation.

$$\mu_{22} = C_2 \rho k^{1/2} l_{\mu,2} \quad (19)$$

where C_1 and C_2 are constants.

For the boundary conditions, the no slip condition is applied at the solid boundary, whereas mean velocity and turbulent kinetic energy gradients are zero on the maximum velocity line and $\theta = 0$ and $\pi/6$ boundaries due to symmetry. On the two radial boundaries ($\theta = 0$ or $30°$), the secondary velocity component V is zero everywhere since the secondary flows can not cross a boundary. However the secondary velocity W on the central boundary may have finite values along these boundary. The boundary conditions for mean axial velocity was imposed by the wall functions on the first string of nodes in the fluid adjacent to the wall. The wall function of axial velocity are obtained from the law of the wall. [9] The wall functions are described by the following equations.

$$U^+ = y^+ \text{ for } 0 \le y^+ < 5$$

$$U^+ = -3.05 + 5.0 \ln y^+ \text{ for } 5 \le y^+ < 30$$

$$U^+ = 5.5 + 2.5 \ln y^+ \text{ for } y^+ < 30$$

$$\text{where } y^+ = \frac{yU^*}{\nu}, \; U^+ = \frac{U}{U^*} \text{ and } U^* = (\tau_w / \rho)^{1/2}. \quad (20)$$

The boundary condition for the turbulent kinetic energy which is imposed at the same nodes is given by the following equation.

$$k = (\frac{\tau_w / \rho}{(C_v C'_d)^{1/2}}) \quad (21)$$

To solve above wall function, updated values of shear stress are used in the main iterative procedure. After each iteration, local values of wall shear stress are computed at the second string of nodes by the following empirical correlation.

$$U = \frac{(\tau_w/\rho)}{(C_v C'_d)^{1/4} (k)^{1/2}} \{\, 2.5 \ln [\, 7.6 \rho y (C_v C'_d)^{1/4} (k)^{1/2} \mu\,]\,\} \quad (22)$$

where C_v and C'_d are turbulent constants. Using the current computed values of U and k, the new shear stress are then used to revise the U and k boundary condition for wall function.

4. Numerical Method

For computation of the solutions of thr-ee-dimensional governing equations, the finite element technique which has been known to be suitable to accurately describes such complex geometry as the fuel bundles. And integral forms are constructed by Galerkin's-weighted residual method. The flow region is divided into triangular element and shape functions of velocity, turbulent kinetic energy, pressure are linear interpolating function and uniquely defined by the values at the nodal points of the element. To solve governing equations, the successive-substitution technique is used. Pressure and velocity field are obtained from momentum equations and then turbulent kinetic energy is solved by the turbulent kinetic energy equation.

5. Result

The geometry tested is shown in figure 1. The rectangular coordinate is used to analyze the secondary flow phenomena of fully developed turbulent flow in the rod bundle channel. Water is used for working fluid. The procedure of calculation is carried out by varying Reynolds number and pitch-to-diameter. And the differnce between isotropic and anisotropic case is shown in the results.

5.1 Effects of Reynold Number and P/D Ratio on the Velocity Field

The distribution of axial velocity and turbulent kinetic energy in figure 3 and figure 2. Contour of predicted secondary velocities are shown in figure 4 with Reynolds number. The maximum secondary velocity is shown on either in the return flow near the wall or adjacent to the maximum axial velocity line. The predicted mean axial velocity distribution for P/D=1.2 is shown in figure 5. The axial velocity increases with going to the MVL. The predicted distribution of turbulent kinetic energy is shown in figure 6. The effects of Reynolds number and P/D on the secondary velocity field are compared in figure 9-14. The friction factor calculated is shown in figure 16 with varying Reynolds number. For a given P/D, friction factor decreases with increasing Reynolds number. For a given Reynolds, friction factor increases with P/D. For a given P/D, the effecfs of increasing Reynolds number on the secondary velocities are illustrated in figure 13 and 14. As can be seen in figure 13, W normalized by U generally becomes increasing with Reynolds number. Figure 15 shows that increasing Reynolds number flatterns the wall shear stress distribution.

5.2 Effect of Anisotropic Eddy Viscosity and Secondary Flow

The predicted secondary flow pattern in a primary flow cell consists of a single cell of secondary flow which transports fluid from the high momentum region near the subchannel center to the low momentum region near the gap via the maximum veocity line boundary with return flow along the rod surface. Secondary flows arise mainly due to anisotropy in the Reynolds stress and then secondary velocities of anisotropic case is higher than isotropic case. And this secondary velocity makes axial velocity higher. Therefore, the effect of secondary flow is evident on the mean axial velocity, turbulent kinetic energy and wall shear stress distribution. It acts on to homogenize wall shear stress along the rod surface by increasing the local value of shear stress, Thus, experimental data on anisotropy factor and secondary velocity distribution are required to explain more realistic flow preditions which ultimately should establish the true role and importance of secondary flows.

6. Conclusion and Discussion

In this study, the secondary flow in the turbulence phenomena is analyzed in infinite triangular array rod bundles. The one-equation turbulence model is used to analyze the turbulence phenomena. From the results of this study, anisotropy eddy viscosity plays important role in the turbulent flow. Hence, the exact anisotropic eddy viscosity model should be new form to analyze the exact pressure field and secondary velocity fieds. The effect of secondary flow and anisotropy is evident on the turbulent flow phenomena but current design methods are usually based on a subchannel mixing technology which involves subchannel-average quantities and does not explicityly recongnize secondary flows. Hence, the turbulence model of the secondary flow is very important in the modeling of exact flow phenomena. Numerical results are partially compared with experimental data and results showed good agreement with experimental data. However, the more experiments are needed because there are no reliable data on the secondary flow.

Reference

1. Kim,Sin. and G.C. Park, *"Analysis of Anisotropic Turbulent Hear Transfer in Nuclear Fuel Bundles,"* 원자력 학회지, 20권, 1호, (1988)
2. S.S Rao. *"The Finite Element Method in Engineering,"*
3. Carajilescov, P., *"Experimental and Analytical Study of Axial Turbulent Flows in an Interior Subchannel of a Bare Rod Bundles,"* PhD thesis, M.I.T., 1975
4. Trupp, A.C. and Aly, A.M.M., *"Predicted Secondary Flows in Triangular Array Rod Bundles," Journal of Fluid Engineering,* Vol.101,(1979)
5. Trupp, A.C. and Azad, R.S., *"The Structure of Turbulent Flow in Triangular Array Rod Bundiles,"* Nuclear Engineering and Design, Vol.32, No.1.(1975)
6. Subbotin, V.I. and Ushakov, P.A., *"Velocity Field of Turbulent Fluid Flow in a Longitudal Streamline of Chusters of Rods,"* United States Atomic Energy Commision,(1971)
7. Talyor, C. and Hughes, T.G., *"Finite Element Programming of the Navier-Stokes Equation,"* Pineridge Press Ltd.,(1981)
8. J.H. Rust, *"Nuclear Power Plant Engineering,"* Haralson Publishing Book Company(1979)
9. J.O. Hinze, *"Turbulence,"* 2nd ed. Mc-Graw Hill Book Company. New York,(1975)
10. A.M.M, Aly, A.C. Trupp, and A.D. Gerrard, *"Measurements and Prediction of Fully Developed Turbulent Flow in an Equilateral Triangular Duct,"* Journal of Heat Transfer, Vol.85,(1978)
11. J. Hejna and F. Mantlik, *"Turbulent Flow in Rod Bundles with Geometrical Disturbance,"* Journal of Heat Transfer and Fluid Flow, Vol.59,(1982)
12. M.J. Crochet and Keunings, *"On Numerical Die Swell Calculation,"* Journal of Non-Newtonian Fluid Mechanics, Vol 10,(1982)
13. W. Slagter, *"Finite Element Solution of Axial Turbulent Flow in a Bare Rod Bundle Using a One-Equation Turbulence Model,"* Journal of Nuclear Science and Engineering, Vol.82,(1982)

Table 1 Constants of Turbulence Model

Ad	0.236
A_μ	0.0186
C1	0.22(isotropic case)
C2	0.22(isotropic case)
Cd	0.416
σ_k	1.53(one equation model)
Cv	0.22
C'd	0.39
C	0.006

NOMENCLATURES

A	element domain
A_d, A_μ	empirical constants
C, C_1, C_2	empirical constants
C_d, C_v, C'_d	
D	diameter of the fuel rod
k	turbulent kinetic energy
$k^+ = k/u*^2$	dimensionless turbulent kinetic energy
L_1, L_2, L_3	shape function
l_d	length scale for dissipation
l_μ	length scale for eddy viscosity
N	approximation polynomial
P	pressure
R	local turbulent Reynolds number
Re	Reynolds number
U	mean axial velocity
U*	friction velocity
x_l	distance from the wall
$\hat{x}_l$	profile length
y^+	dimensionless distance
V	secondary velocity component
W	secondary velocity component
μ	laminar viscosity
ν	kinematic viscosity
μ_{11}	eddy viscosity normal to the wall
μ_{22}	eddy viscosity parallel to the wall
ρ	density of the fluid
σ	laminar Prandtl number
σ_k	Prandtl number for the turbulent kinetic energy
τ_w	shear stress on the wall

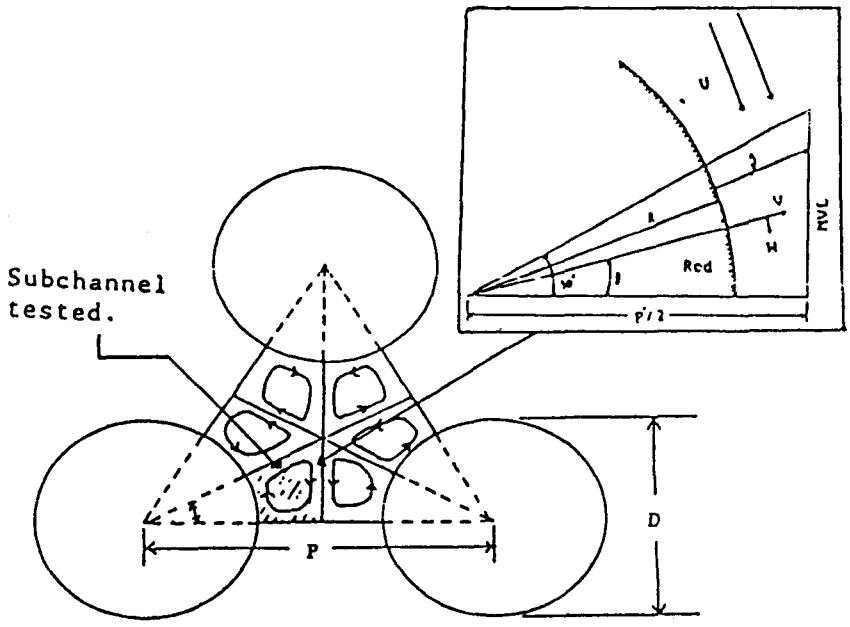

Fig. 1 Rod Bundle Array.

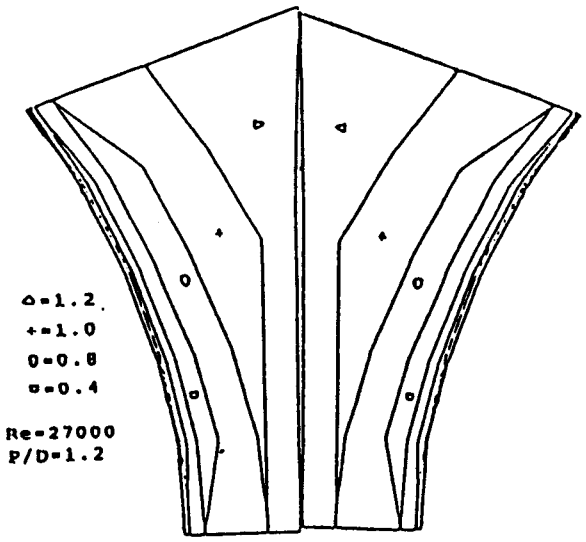

Fig. 2 Countour of U/Uav

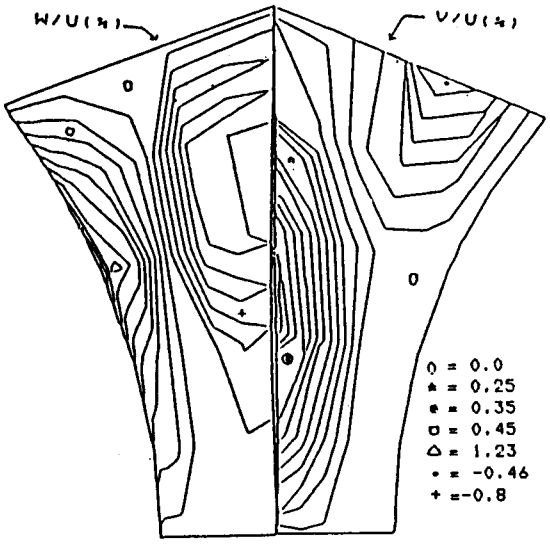

Fig. 4 Countour of Secondary Flow

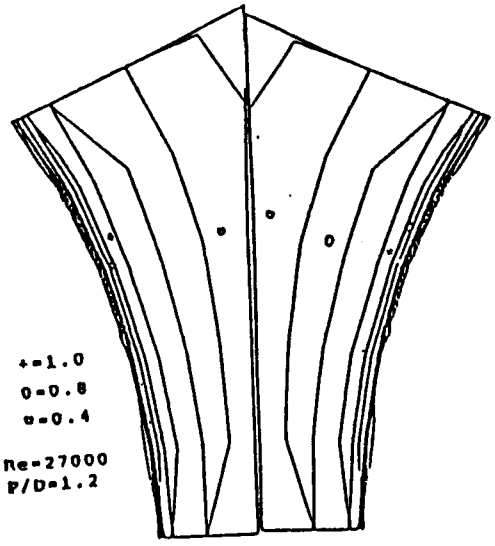

Fig. 3 Countour of *k*/*k*av

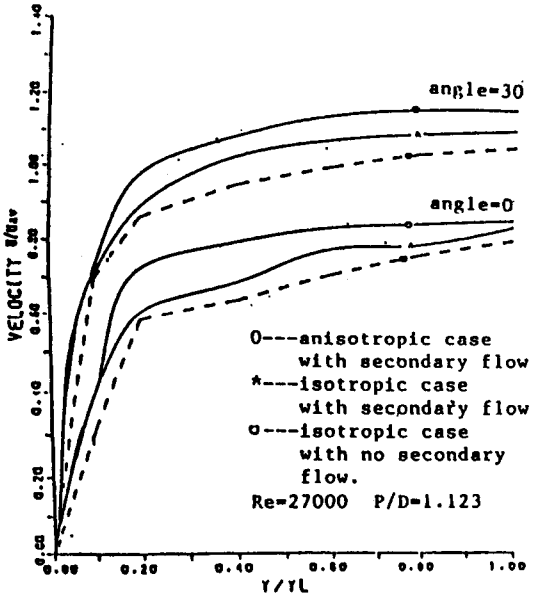

Fig. 5 Mean Axial Velocity U.

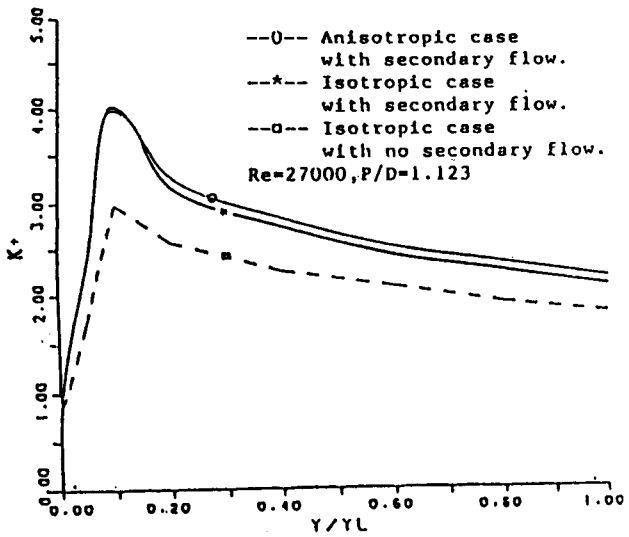

Fig. 6 Turbulent Kinetic Energy k

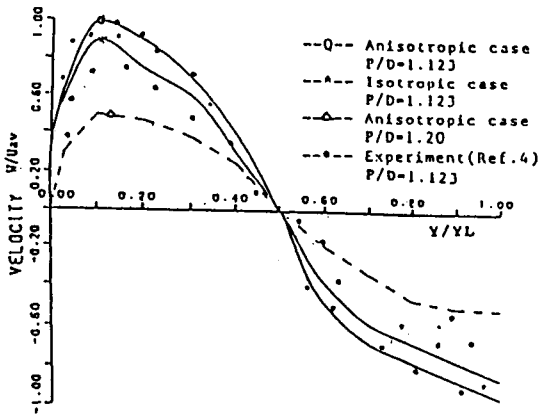

Fig. 7 Secondary Velocity W. vs. P/D

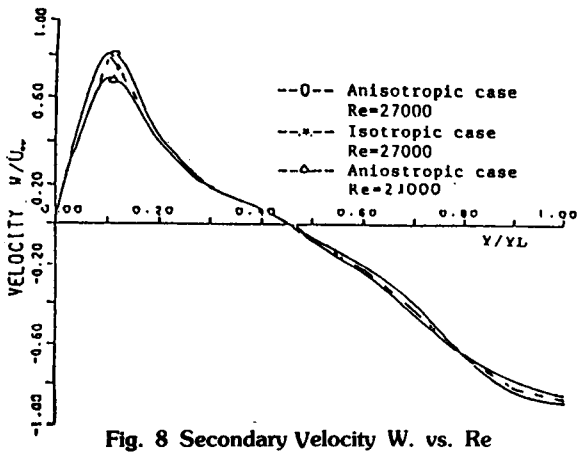

Fig. 8 Secondary Velocity W. vs. Re

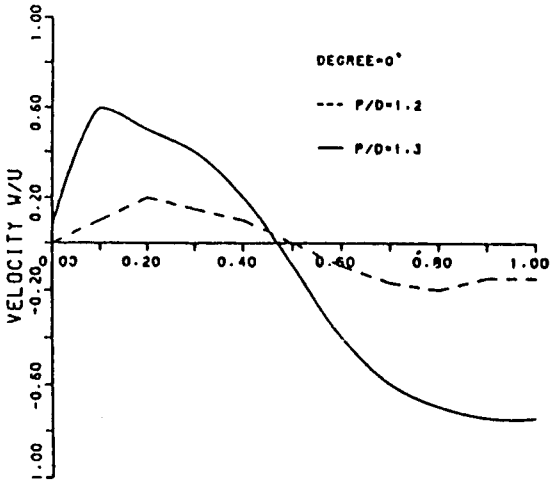

Fig. 9 Velocity Velocity W, RE=27000

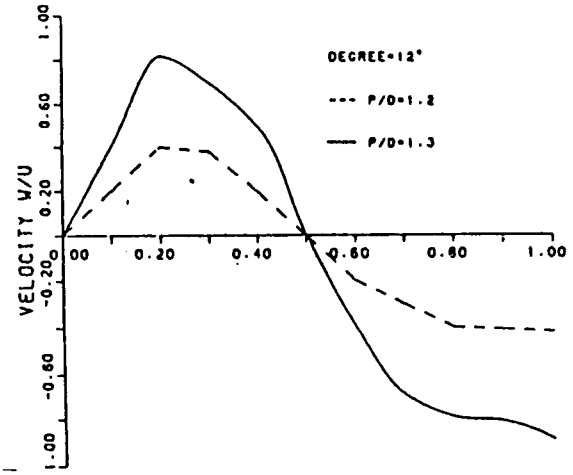

Fig. 10 Secondary Velocity W, RE=27000

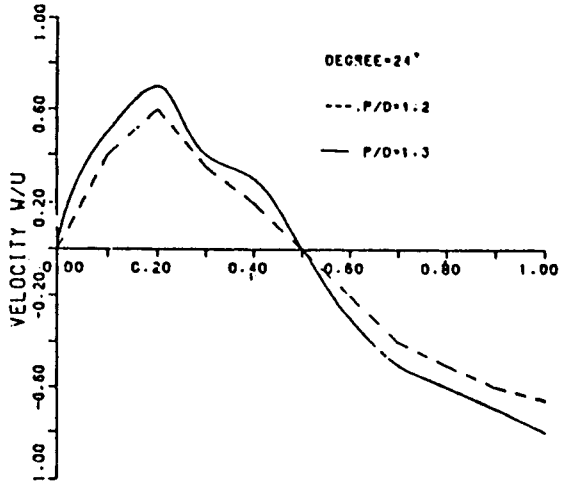

Fig. 11 Secondary Velocity W, RE=27000

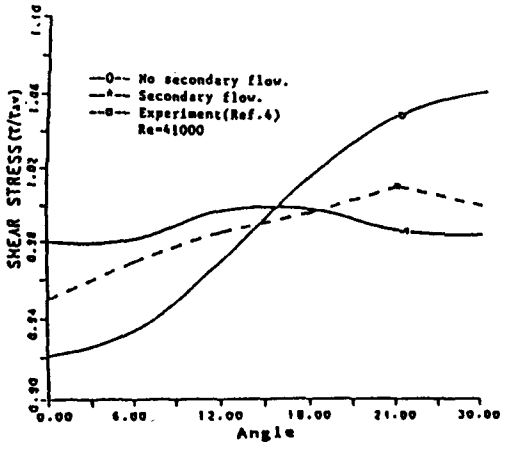

Fig. 15 Shear Stress Distribution

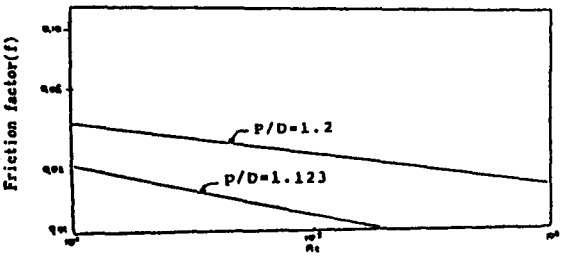

Fig. 16 Friction Factor with Re & P/D